

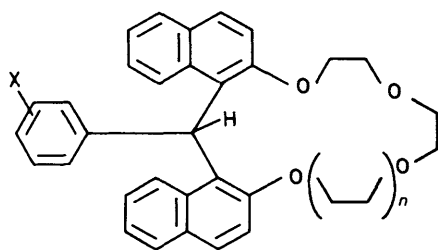
On the Possible Isomerisation Pathway for Triarylmethanes Ar₃CX, including Propeller Crowns

William Clegg and Joyce C. Lockhart*

Department of Inorganic Chemistry, The University, Newcastle upon Tyne, NE1 7RU, UK

The crystal structures of two propeller crown ethers are presented. The properties of the seven propeller crown structures examined to date are compared critically with geometric information retrieved from the Cambridge Crystallographic Database for other Ar₃CX systems. Following the method of Bye, Schweizer, and Dunitz (BSD) each conformation was regarded as a sample point defined by the torsion angles of its three aryl groups, and possible features of the potential energy surface for the interconversion of the propeller isomers were considered graphically. Low-energy stereoisomerisation paths were apparent; the two-ring and one-ring flip transition states of earlier hypotheses did not lie on these paths.

The structure correlation method of inferring low-energy pathways for reaction, given geometric information on a large sample of structures which might lie on or near the reaction co-ordinate, was developed by Bürgi, Murray-Rust, Dunitz, and others,^{1,2} and has provoked much discussion. The structural interconversion of isomers of the three-bladed propeller system Ar₃ZX is a reaction for which suitable information about the ground-state structures of the Ar₃ZX moieties is available. In two recent papers, Bye, Schweizer, and Dunitz³ and Brock, Schweizer, and Dunitz⁴ (BSD) have proposed that maps of structural parameters for Ph₃P-X obtained from the Cambridge Crystallographic Database⁵ may represent low-energy portions of the reaction co-ordinate for stereoisomerisation by coupled torsions of the three aryl rings about their P-C bonds. Only phosphines with unsubstituted rings were considered. Each structure was considered as a point defined in space by the torsion angles of its aryl rings around the C-P bonds. The distribution of the set of such points was considered to define low-energy portions of the reaction co-ordinate. Utilising the high symmetry of the Ph₃PX entity, the sample points were plotted along with symmetry-equivalent points in a hexagonal cell, so that the postulated path for interconversion of the moieties was elegantly revealed (approximately a two-ring flip) in the repeating pattern.



(1)

(2) X = 3, 4, 5 - Trimethoxy, n = 2

(3) X = 2, 6 - Dichloro, n = 1

(4) X = H, n = 2

The dinaphtho propeller crown ethers⁶ [general formula (1)] are an interesting variant on the propeller system Ar₃ZX. The examples we have analysed crystallographically⁶⁻⁸ to date are of one single isomer (B) except in one instance, compound (2), which is isomer (A).⁶⁻⁸ Two new crystal structures [for compounds (3) and (4)] are reported in this paper. The set of crystallographic data for the seven propeller crowns is

examined. A search for further Ar₃CX fragments in the Cambridge database gave a total of 84 fragments, three of which were the crowns published in references 6 and 7. To these, together with the rest of the propeller crowns, the BSD treatment was applied.

Experimental and Calculations

Crowns.—The crowns were prepared by a route described previously.⁶⁻⁸

X-Ray Crystallography.—Crystal data for (3): C₃₅H₃₂Cl₂O₅·CHCl₃, M_r = 722.9. Triclinic, P $\bar{1}$, a = 12.151(1), b = 12.225(1), c = 13.557(1) Å, α = 106.820(4), β = 101.326(5), γ = 109.124(5)°, V = 1 724.3 Å³, Z = 2, D_{calc.} = 1.392 g cm⁻³, F(000) = 748, μ = 0.46 mm⁻¹ for Mo-K α radiation (λ = 0.710 73 Å).

Crystal data for (4): C₃₇H₃₈O₆, M_r = 578.7. Triclinic, P $\bar{1}$, a = 11.521(2), b = 12.245(3), c = 12.352(3) Å, α = 72.52(1), β = 67.77(1), γ = 75.67(1)°, V = 1 520.8 Å³, Z = 2, D_{calc.} = 1.264 g cm⁻³, F(000) = 616, μ = 0.08 mm⁻¹ for Mo-K α radiation.

Data Collection and Processing.—All X-ray data were measured at 293 K with a Siemens AED2 diffractometer. For compounds (3) and (4), the latter are given in square brackets; crystal size 0.35 × 0.46 × 0.50 [0.10 × 0.35 × 0.42] mm, cell parameters from 2 θ values for 32 reflections with 2 θ 20–23° [15–20°]. Intensity measurements in ω/θ scan mode, scan width = 0.725° [1.53°] + α -doublet splitting, scan time = 12–48 s [17.5–70 s], 2 $\theta_{max.}$ = 50° [45°], index ranges: h -14 → 1, k -14 → 14, l -16 → 16 [h -12 → 1, k -13 → 13, l -13 → 13], no significant variation in three standard reflection intensities, no absorption or extinction correction. 7 027 [4 534] Reflections measured, 6 068 [3 977] unique reflections (R_{int.} = 0.016 [0.019]), 4 983 [2 307] with F > 4 σ (F) for structure determination and refinement.

Structure Determination and Refinement.⁹—Multisolution direct methods, blocked-cascade least-squares refinement to minimise $\Sigma w\Delta^2$, $\Delta = |F_o| - |F_c|$, $w^{-1} = \sigma^2(F) + gF^2$, g = 0.000 39 [0.000 35]. Anisotropic thermal parameters for all non-hydrogen atoms, hydrogen atoms included with constraints: C-H = 0.96 Å, H-C-H = 109.5°, aromatic H on C-C-C external bisectors, U(H) = 1.2 U_{eq}(C). Parameters refined 415 [388], R = 0.050 [0.077], R_w = ($\Sigma w\Delta^2 / \Sigma wF_o^2$)^{1/2} = 0.073 [0.084], max. shift/e.s.d. = 0.049 [0.031], mean = 0.015 [0.005], slope of normal probability plot = 2.10 [2.08], no significant features in a final difference synthesis, scattering factors from reference 10. Co-ordinates are given in Tables 1 and 2; bond

Table 1. Atomic co-ordinates ($\times 10^4$) for (3)

	x	y	z
O(1)	4 230(1)	2 492(1)	7 627(1)
C(2)	4 226(3)	1 977(3)	8 447(2)
C(3)	4 124(3)	670(3)	7 991(3)
O(4)	5 192(2)	593(2)	7 773(2)
C(5)	5 215(3)	509(3)	6 704(2)
C(6)	6 353(3)	392(4)	6 580(3)
O(7)	7 430(2)	1 386(3)	7 346(2)
C(8)	8 182(3)	2 232(4)	6 975(3)
C(9)	7 904(3)	3 317(4)	7 018(3)
O(10)	6 793(2)	2 928(2)	6 148(2)
C(11)	6 572(3)	3 948(3)	6 072(3)
C(12)	5 423(2)	3 516(3)	5 174(3)
O(13)	4 396(1)	3 210(2)	5 562(1)
C(14)	3 318(2)	3 135(2)	4 955(2)
C(15)	2 453(2)	3 246(2)	5 458(2)
C(16)	2 651(2)	3 511(2)	6 669(2)
C(17)	3 971(2)	4 272(2)	6 452(2)
C(18)	4 652(2)	3 776(2)	7 958(2)
C(19)	5 824(2)	4 543(3)	8 749(2)
C(20)	6 307(2)	5 796(3)	9 027(2)
C(21)	5 658(2)	6 373(2)	8 538(2)
C(22)	6 135(3)	7 679(2)	8 835(2)
C(23)	5 508(3)	8 232(2)	8 368(2)
C(24)	4 364(2)	7 488(2)	7 559(2)
C(25)	3 868(2)	6 216(2)	7 242(2)
C(26)	4 484(2)	5 604(2)	7 729(2)
C(27)	3 081(2)	2 907(3)	3 836(2)
C(28)	2 004(3)	2 823(3)	3 229(2)
C(29)	1 098(2)	2 962(2)	3 701(2)
C(30)	-6(3)	2 925(3)	3 088(2)
C(31)	-884(3)	3 055(3)	3 537(3)
C(32)	-694(3)	3 220(3)	4 623(3)
C(33)	360(2)	3 266(3)	5 249(2)
C(34)	1 314(2)	3 157(2)	4 820(2)
C(35)	1 912(2)	2 428(2)	6 950(2)
C(36)	1 495(2)	2 715(2)	7 842(2)
C(37)	828(2)	1 822(3)	8 185(2)
C(38)	524(3)	584(3)	7 609(3)
C(39)	892(2)	248(3)	6 721(2)
C(40)	1 578(2)	1 155(2)	6 402(2)
Cl(41)	1 771(1)	4 263(1)	8 573(1)
Cl(42)	2 042(1)	606(1)	5 295(1)
C(43)	8 067(3)	1 977(4)	9 772(3)
Cl(44)	7 141(1)	2 097(1)	10 592(1)
Cl(45)	9 260(1)	3 436(1)	10 131(1)
Cl(46)	8 694(1)	904(1)	9 894(1)

lengths and angles are as expected for aryl group and crown ethers, and have been deposited as supplementary data.*

Search of Database and Preparation of Data.—The May 1986 version of the Cambridge Crystallographic Database available in the CDS system at Daresbury was used for the search. A total of 84 suitable Ar_3CX fragments was discovered. Some geometric calculation on the entries was carried out using the program VIEW on a VAX at Daresbury.† Most of the calculations were done using the program MODEL¹¹ on a VAX 11/780 at Newcastle. No attempt was made to restrict the data to unsubstituted or symmetrically substituted aryl rings, as was done by BSD, since the Ar_3PX data in virtually all the cases they considered showed considerable deviations from the idealised

Table 2. Atomic co-ordinates ($\times 10^4$) for (4)

	x	y	z
O(1)	5 615(3)	1 958(3)	4 141(3)
C(2)	4 390(5)	2 308(5)	4 010(5)
C(3)	4 559(6)	3 024(6)	2 768(5)
O(4)	3 339(4)	3 343(4)	2 639(4)
C(5)	3 354(7)	3 685(6)	1 448(6)
C(6)	3 452(9)	4 938(8)	875(6)
O(7)	2 413(6)	5 715(5)	1 246(5)
C(8)	2 327(8)	6 121(7)	2 178(7)
C(9)	3 121(9)	7 044(8)	1 890(10)
O(10)	4 336(6)	6 431(6)	1 982(7)
C(11)	5 061(6)	7 049(6)	1 977(9)
C(12)	6 267(7)	6 508(6)	2 143(7)
O(13)	6 938(4)	5 710(4)	1 484(4)
C(14)	8 158(6)	5 216(5)	1 558(6)
C(15)	8 535(6)	4 070(5)	1 251(5)
O(16)	7 775(3)	3 263(3)	2 196(3)
C(17)	8 082(5)	2 133(4)	2 088(5)
C(18)	8 174(4)	1 255(4)	3 074(4)
C(19)	8 079(5)	1 449(4)	4 279(4)
C(20)	6 914(4)	1 049(4)	5 327(4)
C(21)	5 726(5)	1 282(4)	5 223(4)
C(22)	4 665(5)	864(4)	6 169(5)
C(23)	4 816(5)	253(4)	7 230(5)
C(24)	5 979(5)	37(4)	7 426(5)
C(25)	6 088(5)	-547(5)	8 562(5)
C(26)	7 197(6)	-714(5)	8 766(5)
C(27)	8 259(5)	-289(5)	7 838(5)
C(28)	8 176(5)	269(4)	6 735(5)
C(29)	7 042(5)	452(4)	6 471(4)
C(30)	8 199(5)	1 910(5)	999(5)
C(31)	8 434(5)	813(5)	873(5)
C(32)	8 549(5)	-132(5)	1 843(5)
C(33)	8 795(5)	-1 286(5)	1 715(5)
C(34)	8 944(5)	-2 188(5)	2 631(6)
C(35)	8 841(5)	-1 996(5)	3 726(6)
C(36)	8 580(5)	-885(5)	3 874(5)
C(37)	8 423(4)	90(4)	2 945(4)
C(38)	8 333(5)	2 601(4)	4 269(4)
C(39)	9 564(6)	2 831(5)	3 825(5)
C(40)	9 850(9)	3 833(7)	3 876(7)
C(41)	8 909(10)	4 627(7)	4 372(6)
C(42)	7 664(8)	4 439(6)	4 840(5)
C(43)	7 378(6)	3 428(5)	4 766(5)

C_{3v} frame. Very few of the symmetrically substituted Ar_3CX molecules examined have attained C_{3v} symmetry, the exceptions being the $\text{Ph}_3\text{C}-\text{Cl}$ and $-\text{Br}$ molecules. Comment is made later about the asymmetrically substituted compounds. In any case it was necessary to replace the $\text{C}-\text{X}$ vector, as recommended by BSD, in order to provide a consistent set of torsion angles, calculated to the same reference, which is a dummy atom at the centroid of the apex (α) carbons of the aryl ring. The α -C atoms (called AR in the Tables) were labelled A, B, and C in a clockwise order viewed down the $\text{X}-\text{C}$ direction. For any data set for which the twist of the rings was not clockwise, co-ordinates for the molecule related through a crystallographic centre of symmetry were used instead. Using a dummy atom D at the centroid of C_A , C_B , and C_C , the torsion angles $\text{D}-\text{CEN}-\text{C}(\text{AR})-\text{C}_i$ ($i = 1, 2$) involving C_i , the *ortho*-carbons, were calculated, and the best estimate of the ring torsion angle was taken as $\varphi = (t_1 + t_2 + 180)/2$. Then the phenyl group with the largest torsion angle was taken as ring A, and the rings B and C were assigned following the clockwise order. The torsion angles $\varphi_A\varphi_B\varphi_C$ were used to calculate hexagonal co-ordinates using equations (1)–(3), and the quantity d (a measure of the deviation from ideal propeller symmetry) was calculated from equation (4).

* Supplementary data (see section 5.6.3 of Instructions for Authors, in the *J. Chem. Soc., Perkin Trans. 2*, 1987, issue 1, pp. xvii–xix). Lists of bond lengths and angles have been deposited at the Cambridge Crystallographic Data Centre.

† CDS System provided by the S.E.R.C. at Daresbury.

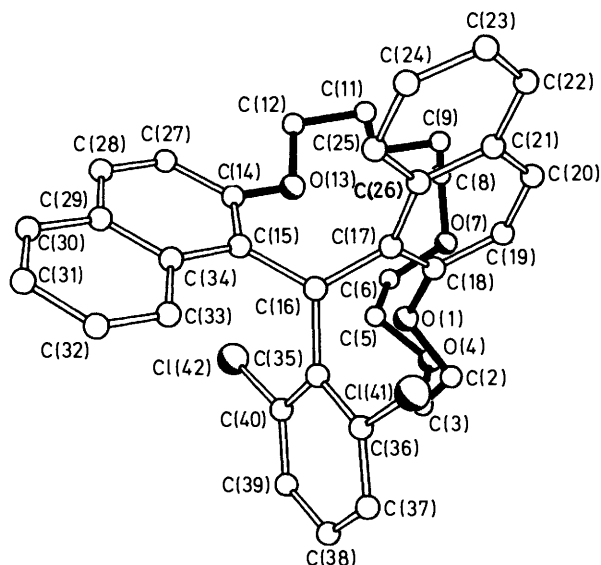


Figure 1. Molecular structure of (3) projected on the reference plane; propeller section with open bonds, crown ring with filled bonds

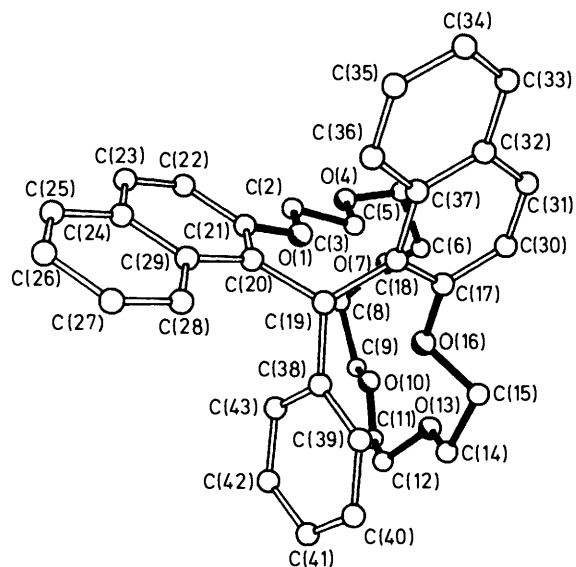


Figure 2. Molecular structure of (4) projected on the reference plane; propeller section with open bonds, crown ring with filled bonds

Results and Discussion

Figure 1 shows the molecular structure of (3) and Figure 2 that of (4), both projected on the plane of the three C atoms bonded to the central propeller carbon, C(16) or C(19).

The projections demonstrate clearly that the propeller skeleton takes up the conformation denoted B, which has now been observed for six of the total of seven structures so far determined. The inference is that this generally constitutes the lowest-energy isomer. The torsion angles round the crown ether strands given in Figure 3 and 4 are aaa , $g^+g^+g^-$, g^-g^+a , ag^-a , ag^+a for (4) and ag^+a , ag^-g^+ , ag^-a , g^-g^+a for the five-donor crown (3). The aaa segment next to naphthyl oxygen (O1) is unusual. For the 36 ether segments observed in these seven structures and the two-bladed propeller in reference 7, although eight different conformations are found, 21 of these are of the $ag^\pm a$ type. There are only three in which the C-C torsion is *anti*,

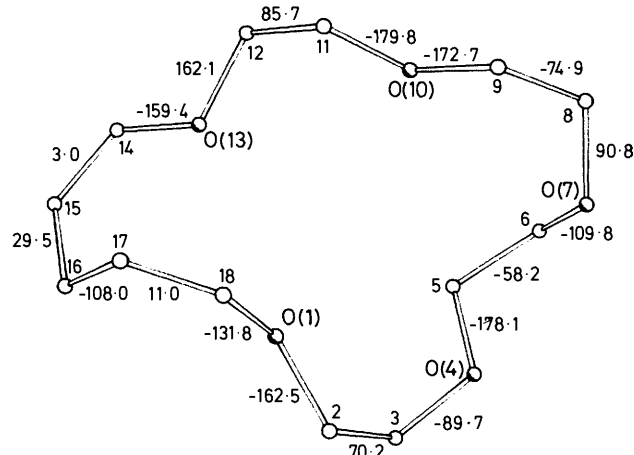


Figure 3. Torsion angles in (3): carbon atoms are labelled by number only

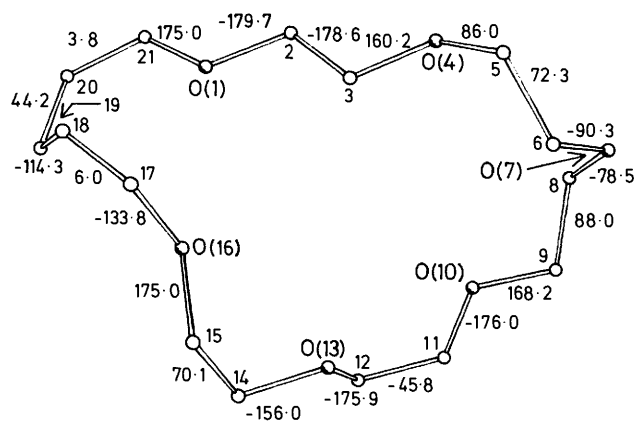


Figure 4. Torsion angles in (4): carbon atoms are labelled by number only

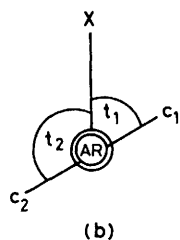
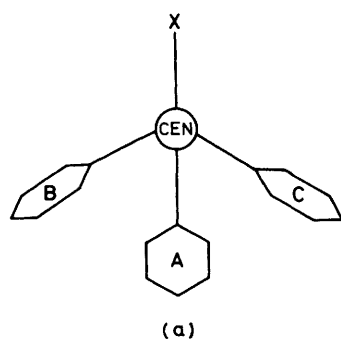
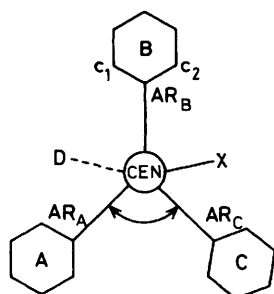
viz. two aaa and one aag^- segment, and these occur exclusively in segments next to the naphthyl rings, for which solution n.m.r. measurements also suggest a small *trans* population in equilibrium with preponderant *gauche* forms.⁸ That the ether geometry is variable while the propeller geometry is not shows that fluxionality is preserved in the ether strand while the propeller part presents a more rigid barrier to isomerisation. Indeed, the activation energy barriers to propeller flipping are from 10–19 kcal mol⁻¹ in this series.⁸

An idealised Ph₃C- structure is given in Figure 5, which shows the convention of labelling the torsion angles which we follow from the BDS paper. Analysis of propeller crown data shows no clear difference between the unusual isomer and the other six, but the geometrical parameters for this isomer are at the extremes of the range. The parameters (recorded in the supplementary data) are the C.S.S.R. registration number except for propeller crowns not yet included, the three torsion angles $\phi_A\phi_B\phi_C$, the attached atom X, the distance from the central carbon (CEN) to X, mean distance from CEN to the attached aryl carbons, the mean angle between attached aryl carbons and CEN, the mean distance from the dummy (centroid) atom to the attached aryl carbons, and the distance from the dummy to the central carbon (CEN). A definition is shown in Figure 6 of each geometrical feature.

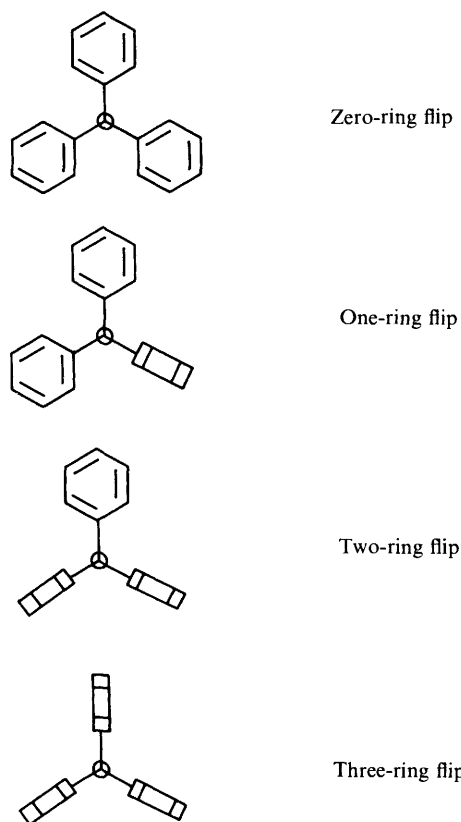
The data were arranged in sets according to the attached atom X, with one 'miscellaneous' set for F, P, S, Cl, Br, and Sn, for each of which there are only a few examples. Statistics for average geometrical parameters for the individual sets and for

Table 3. Average parameters for atom types X

X	Torsions			CEN-X	CEN-AR	ANGLE	D-AR
	φ_A	φ_B	φ_C				
Misc.	53.7	43.5	39.6	1.703	1.521	112.5	1.458
S.D.	13.0	9.8	17.9	0.64	0.032	3.2	0.012
H	45.8	29.4	35.8	0.97	1.529	114.6	1.478
S.D.	4.6	9.0	4.4	0.02	0.004	1.2	0.017
O	70.3	31.9	3.5	1.450	1.539	111.2	1.461
S.D.	15.5	19.2	25.7	0.01	0.01	1.0	0.012
N	60.6	43.0	17.9	1.484	1.541	110.1	1.460
S.D.	13.1	16.1	19.9	0.022	0.004	1.2	0.006
C	69.9	42.1	7.6	1.557	1.545	109.9	1.460
S.D.	14.7	10.6	25.0	0.03	0.009	1.0	0.011

**Figure 5.** (a) Labelling of the triarylmethanes as in reference 3. (b) Definition of the torsion angles of one aryl ring relative to the two *ortho*-carbons C_1 and C_2 **Figure 6.** Definition of terms used

the entire group of propellers are in Table 3. The propeller crowns had a large average angle AR-CEN-AR and the distance D-CEN was very low, indicating a general flattening of the propeller in the crowns. When the five sets of data in Table 3 are compared, it is seen that ANGLE correlates with X-CEN (inversely). The average geometry indicates the C-C compounds to be nearest to tetrahedral geometry, and the C-H most

**Figure 7.** Idealised transition states formerly proposed for the 0, 1, 2, and 3 ring flip mechanisms (as labelled) of three-bladed propellers

distorted to trigonal planar. Further discussion of the observed geometries follows the consideration of the low-energy pathway.

The derived set of hexagonal co-ordinates X_H , Y_H , and Z_H , along with the 'distance' d were obtained from equations (1)–(4), as described by BSD.

$$X_H = (2\varphi_A - \varphi_B - \varphi_C)/3 \quad (1)$$

$$Y_H = (\varphi_A + \varphi_B - 2\varphi_C)/3 \quad (2)$$

$$Z_H = (\varphi_A + \varphi_B + \varphi_C)/3 \quad (3)$$

$$d = (X_H^2 + Y_H^2 - X_H Y_H)^{\frac{1}{2}} \quad (4)$$

Isomerism in three-bladed propellers is thought to occur by correlated rotations of the aryl rings (blades), and four general

mechanisms proposed first by Kurland, Shuster, and Colter,¹² have been investigated by empirical theory and experiment, particularly by Mislow and co-workers.¹³ The four mechanisms consider zero, one, two, or all three of the aryl rings to 'flip', that is to twist around the AR-CEN bond perpendicular to the reference plane, while the remaining rings rotate in the opposite direction through the reference plane. The mechanisms are schematically shown in Figure 7, which shows the previously suggested¹³ idealised transition states, with the flipping rings perpendicular to the plane of the paper (the reference plane is coincident) and the remaining rings lying on the plane.

For an unsubstituted Ph_3CX molecule, (assuming *R* or *S* chirality at the methine) the rings can adopt two propeller conformations of opposite helicity, called here Δ or λ . The hexagonal mapping shown in Figure 8(a) is a representation of the possible ways in which the two forms can interconvert. Each vertex represents a λ or a Δ form, and each connecting edge represents a path for their interconversion by the two-ring flip (the most commonly suggested path). Each vertex is three-connected, each line representing one of the three possible two-ring flips for that form. The mapping resembles the hexagonal representation produced in the BSD paper,³ but it should be noted that Figure 8(a) has no direct physical meaning, while the BSD map (see later Figure 11 for a similar one) is a graph of geometries actually observed, and the connecting lines are not straight. The mapping is also equivalent to the Mislow cube representation which we have used in studies of correlated rotation of propeller crowns,^{7,8} since each vertex of the cube is also three-connected. The mapping in Figure 8(a) is strictly

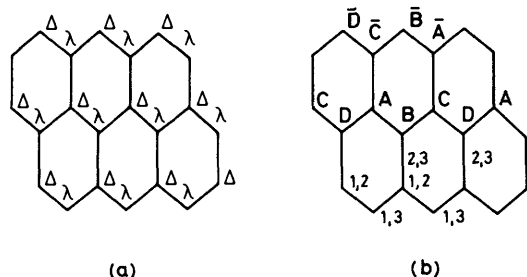


Figure 8. Hexagonal mapping representing the symmetry-related interconversion of λ to Δ forms of Ph_3CX ; (b) a restricted version of this mapping applicable to the propeller crowns

applicable to the unsubstituted, perfectly symmetrical Ph_3CX molecules, of which but five emerged in our study. However, appropriate restricted versions of this mapping [Figure 8(b)] can be used for systems with less symmetry. There are equivalent Mislow cube representations appropriate to two-ring flips in propeller crowns, and Figure 8(b) is labelled to show the correspondence between vertices and edges. The eight isomers shown in the hexagonal mapping in Figure 8(b) have alternate helicities. Each is connected by three different two-ring flips to three different isomers, of opposite helicity. Few of the structures extracted from the database had substituted aryl rings, insufficient for a separate analysis. None of these was in any case particularly distorted from C_{3v} symmetry. The molecules showing greatest distortions from C_{3v} symmetry were crowded and polyphenyl substituted, or contained Ar_3CO -residues (especially where O was part of a carbohydrate).

We felt justified in applying the same treatment to all the fragments, since C_{3v} symmetry was so exceptional, although strictly one should differentiate the three pathways of the BSD diagram which can lead to three different isomers for systems without C_{3v} symmetry.

The hexagonal co-ordinates were plotted in a hexagonal unit cell with symmetry-related points included, as shown in Figures 9 and 10, from different viewpoints. In Figure 9 (drawn on the same basis as Figure 3 of reference 3) the apparent path traced out by the points is curved, so that it does not follow the edges of a hexagon, but deviates alternately to the left and to the right of the edges, a feature much more prominent in this map than in the BSD map.³ The most heavily populated portion of the composite map in Figure 9 is that corresponding to the molecules with near C_{3v} symmetry; these are mostly the set where X is a second-row atom, or hydrogen.

The next most heavily populated portion of the map is essentially the route-line traced parallel to each hexagon edge. This is most clearly seen in Figures 11 and 12, which contain the data for $X = \text{C}$ and $X = \text{O}$ respectively. The route falls between the points (marked in the Figures) which would correspond to the putative transition states for the idealised two- and one-ring flips. The points in this region seem to constitute another minimum in the potential energy surface; indeed a histogram of the angles ϕ_A is clearly bimodal with peaks at $45\text{--}50^\circ$ and at 85° , and troughs at $0\text{--}40^\circ$ and at 75° . The least populated part of Figures 11 and 12 is quite clearly the region between molecules close to C_{3v} symmetry and those represented by the

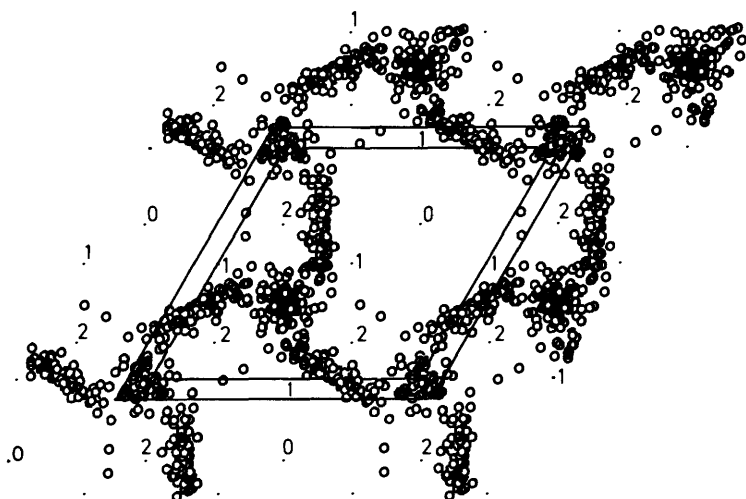
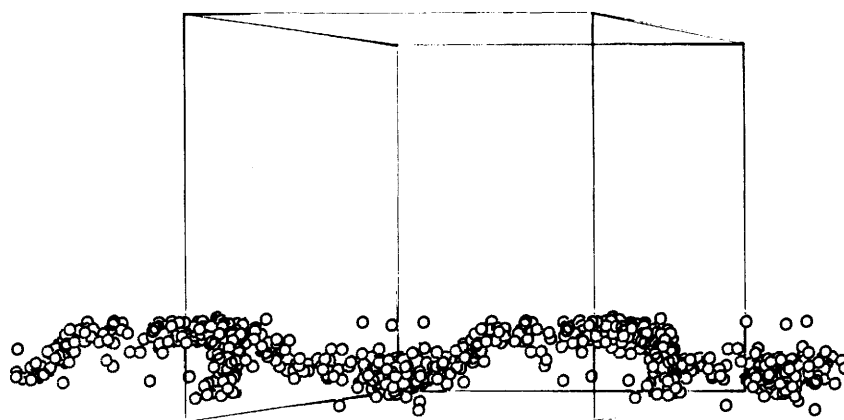
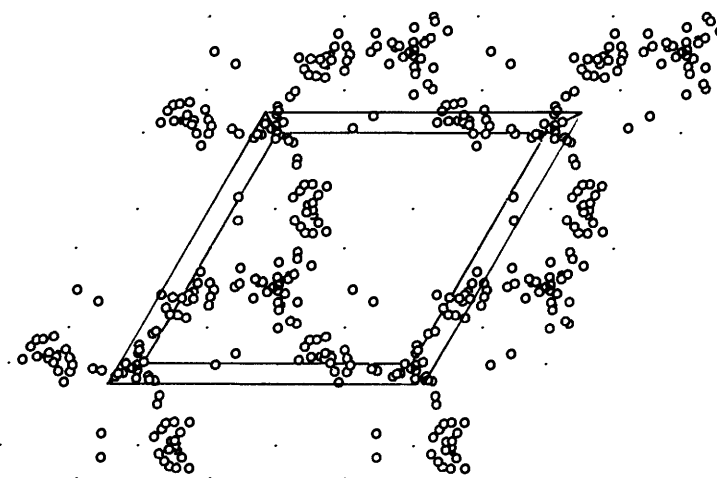


Figure 9. The motif obtained from the hexagonal co-ordinates seen in perspective down the hexagonal axis with symmetry-related points included (with $0 \leq Z \leq 60^\circ$). The idealised transition states of Figure 7 are labelled 0, 1, and 2. The three-ring flip transition state lies at the cell corners and symmetry-related positions

Table 4. Geometries closest to the two-ring flip (ring A flat)*

		φ_A	φ_B	φ_C	CEN-AR			D-AR			AR-CEN-AR		
					A	B	C	A	B	C	AB	AC	BC
Mean	X = C	85.01	23.02	6.19	1.541	1.545	1.559	1.509	1.439	1.430	112.7	111.3	104.4
	S.D.	1.75	25.4	24.4	0.005	0.009	0.017	0.072	0.053	0.020	1.96	1.83	1.4
Mean	X = O	85.06	19.89	-12.2	1.537	1.545	1.545	1.506	1.441	1.446	113.3	113.2	106.2
	S.D.	1.57	15.5	22.6	0.017	0.010	0.015	0.016	0.022	0.018	1.8	2.1	1.2
Mean	X = C, O, N	85.0	22.4	-3.5	1.539	1.545	1.552	1.507	1.440	1.437	113.0	112.2	105.2
	S.D.	1.6	20.5	24.3	0.012	0.009	0.017	0.051	0.039	0.020	1.8	2.1	1.6

* The data are tabulated as: φ_A , φ_B , and φ_C are the torsion angles A, B, C as defined by BDS. X is the atom attached to the central atom of the propeller. CEN-X is the distance from central atom CEN to X. CEN-AR is the mean distance from CEN to the (bonded) aryl ring carbon. AR-CEN-AR is the mean angle from bonded aryl carbons to the centre, and AB, AC, etc., denote the ring to which the bonded carbon belongs. D-AR is the mean distance from the dummy centroid to the AR atoms (labelled A, B, C according to which ring they are attached to).

**Figure 10.** The points of Figure 9 seen from the side**Figure 11.** As Figure 9 but showing only points for molecules with X = O

route-line so that, on this analysis, there would be two transition states for each isomerisation, with a low-energy intermediate lying between them. Figure 10 also shows the empty regions. An alternative explanation, that the molecules in the database do *not* constitute a random population of triarylmethanes, would negate our analysis.

From the data, the 19 fragments containing one flat A ring ($80 < \varphi_A < 90^\circ$) (as required for the two-ring flip mechanism) were extracted, tabulated for X = N, O or C, and a more detailed analysis of their geometry undertaken. Details are in Table 4. The mean distance CEN-AR_A is marginally smaller than CEN-AR_B or AR_C, differing by about half of the

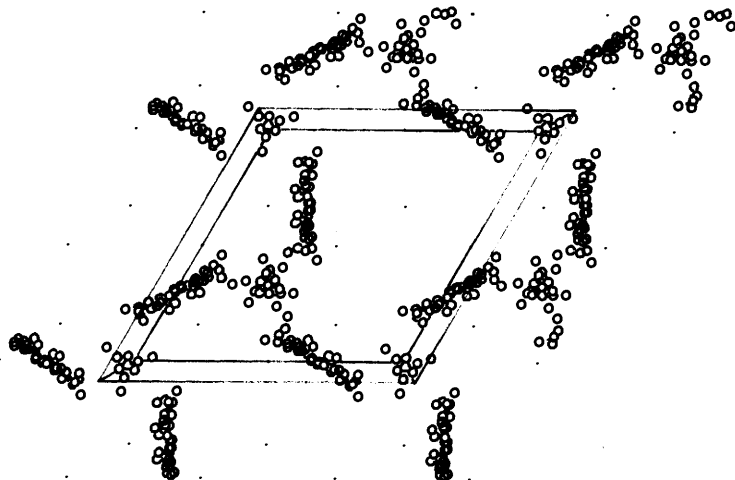


Figure 12. As Figure 9 but showing only points for molecules with $X = C$

standard deviation. The distortion of each structure from ideal symmetry may be gauged from $D-AR_A$, $D-AR_B$, and $D-AR_C$ in the same Table, where the respective lengths consistently show the flat ring (see Figure 5) to be further from the centroid than are the other two rings. The angles $AR-CEN-AR$ are also given. The angle $AR_B-CEN-AR_C$ is expected to be smaller than the other two, because of van der Waals repulsion involving the flat aryl ring (see Figure 5), and this is found with few exceptions. These fragments are close to the line representing the intermediate. The asymmetry of these structures is a phenomenon which might be anticipated from the asymmetry of their environments. Tilt and asymmetry of methyl and other groups in asymmetric environments have been observed by microwave spectroscopy and reproduced in *ab initio* calculations.¹⁴ The methyl C-H *trans* to a lone pair (*e.g.* in methylamine) is longer than the other two C-H bonds. The bias of the compounds with $X = O$, N has a similar origin. The bias for compounds with $X = C$ must derive from asymmetric substitution on that carbon.

Conclusion

The triarylmethanes follow a reaction path different from that for the phosphines. The idealised transition states previously considered for the two- and one-ring flip seem to be high-energy structures not on the reaction co-ordinate. The hypotheses of the two- or one-ring flip probably fail in considering any two rings to behave identically. In the real molecules each ring presumably behaves individually, although their motions are coupled. In addition to torsional changes, bond lengths and angles appear to alter to minimise strain. Molecules such as these in Table 4 with one flat ring constitute low-energy intermediates, the transition states lying between these and C_{3v} symmetry.

Acknowledgements

We thank the S.E.R.C. for crystallographic facilities and for the use of CDS, also NUMAC for computing facilities, Dr. M. B. McDonnell for crown (4), and Mrs. L. Cook for crown (3).

References

- 1 H. B. Bürgi, *Inorg. Chem.*, 1973, **12**, 2321.
- 2 P. Murray-Rust, H. B. Bürgi, and J. D. Dunitz, *J. Am. Chem. Soc.*, 1975, **97**, 921.
- 3 E. Bye, W. B. Schweizer, and J. D. Dunitz, *J. Am. Chem. Soc.*, 1982, **104**, 5893.
- 4 C. P. Brock, W. B. Schweizer, and J. D. Dunitz, *J. Am. Chem. Soc.*, 1985, **107**, 6964.
- 5 Cambridge Crystallographic Data Centre, University Chemical Laboratories, Cambridge. F. H. Allen, S. Bellard, M. D. Brice, B. A. Cartwright, A. Doubleday, H. Higgs, T. Hummelink, B. G. Hummelink-Peters, O. Kennard, W. D. S. Motherwell, J. R. Rodgers, and D. G. Watson, *Acta Crystallogr., Sect. B*, 1979, **35**, 2331.
- 6 J. C. Lockhart, M. B. McDonnell, and W. Clegg, *J. Chem. Soc., Chem. Commun.*, 1984, 365.
- 7 W. Clegg, J. C. Lockhart, and M. B. McDonnell, *J. Chem. Soc., Perkin Trans. 1*, 1985, 1019.
- 8 J. C. Lockhart, M. B. McDonnell, W. Clegg, and M. N. S. Hill, *J. Chem. Soc., Perkin Trans. 2*, 1987, 639.
- 9 G. M. Sheldrick, 'SHELXTL, an integrated system for solving, refining and displaying crystal structures from diffraction data.' Revision 5. University of Göttingen, 1985.
- 10 International Tables for X-ray Crystallography, Vol. IV, pp. 99, 149. Kynoch Press, Birmingham, 1974.
- 11 Chemgraf, created by E. K. Davies, Chemical Crystallography Laboratory, Oxford University, developed and distributed by Chemical Design Ltd., Oxford.
- 12 R. J. Kurland, I. K. Shuster, and A. K. Colter, *J. Am. Chem. Soc.*, 1965, **87**, 2279.
- 13 K. Mislow, *Acc. Chem. Res.*, 1976, **9**, 26.
- 14 E. Flood, P. Pulay, and J. E. Boggs, *J. Am. Chem. Soc.*, 1977, **99**, 5570.

Received 3rd November 1986; Paper 6/2133